Available online freely at www.isisn.org

Bioscience Research

Print ISSN: 1811-9506 Online ISSN: 2218-3973

Journal by Innovative Scientific Information & Services Network

RESEARCH ARTICLE BIOSCIENCE RESEARCH, 2020 17(1): 467-478. **OPEN ACCESS**

Assessment of Sentinel-2 data capabilities for vegetation physiological parameters retrieving in the Nile Delta

Eslam Farg*[1], Khaled A. Abutaleb [1,2,3], S. M. Arafat [1], Mohamed M. El Sharkawy[4], and Mohsen Nabil [1,5,6]

[1] National Authority for remote sensing and space sciences NARSS, **Egypt**
[2] Institute for Soil, Climate & Water, ARC, Pretoria, **South Africa**
[3] University of Witwatersrand, Johannesburg, **South Africa**
[4] Soil and Water Dept., Faculty of Agriculture, Beni-Suef University, **Egypt**
[5] State Key Laboratory of Remote Sensing Science, Aerospace Information Research Institute, Chinese Academy of Sciences, Beijing 100101, **China**
[6] University of Chinese Academy of Sciences, Beijing 100049, **China**

***Correspondence:** efargnarss@gmail.com **Received 30-12-2019, Revised: 08-03-2020, Accepted: 10-03-2020 e-Published: 15-03-2020**

Vegetation bio-physiological parameters are essential in crop management for both agricultural decision-makers and stockholders. Remote sensing has been used for estimation growth indicators during different growth stages. The main objective of the current study is the assessment of Sentinel-2 satellite data for retrieving the Leaf Area Index (LAI) using two different algorithms the Multi-Linear Regression (MLR) and the Neural Networks (NNs) to compare their results with standard method impeded in the SNAP software for calculating LAI. In this study, field measurements of 106 samples of potato and wheat crops were carried out at three different dates during the growing season of 2017. Field measurements included spectral reflectance and LAI. Moreover, the field measurements synchronized to the Sentinel-2 satellite images acquisition at three different growth stages. Preliminary statistical analysis applied to both collected field data and mapped biophysical parameters for identifying data outliers. Furthermore, Stepwise MLR and Gauss-Newton NNs used to model and predict LAI from the satellite data. The NNs showed a higher coefficient of determinations (R^2) than MLR with R^2 = 0.94 and 0.89, respectively, between the predicted and field-measured LAI. Concluding that NNs significantly enhanced the prediction accuracy of LAI using Sentinel-2 data compared to the linear regression methods.

Keywords: MLR, LAI, Sentinel-2, Neural networks

INTRODUCTION

Implementation of new technologies such as remote sensing data and Geographical Information System (GIS) are required for best on-farm management and practices to achieve the optimal crop productivity. Remote sensing applications in agriculture depend on the spectral reflectance of the vegetation canopy and the soil background. Remote sensing techniques offer solutions to the limitations and shortcomings of conventional methods for estimating and retrieving important biophysical and biochemical parameters for agriculture development and crop monitoring. It provides near real-time information such as crop water use, crop coverage, and field spatial variability.

Methods for measuring LAI could be divided into two main categories: direct methods and

indirect methods. According to (Jonckheere et al., 2004), the direct methods are the most accurate and can be used for calibrating the indirect methods. However, they are destructive, economically expensive, time-consuming, and not feasible for high temporal and large-scale studies. In contrast, the indirect methods are non-destructive, economically feasible for large areas, and more compatible with the vegetation cover long-term monitoring due to their high spatial and temporal resolution. An example of the direct method is remote sensing, which has been widely used for LAI estimation. Blanco & Vin (2003), built three mathematical equations for estimating LAI from the length, width, or length * width of the actual leaf area. The authors also concluded that the equations used only one leaf dimension (width or length) were more correlated to LAI in comparison to the equation used both (width and length). There are two main approaches to drive LAI from remotely sensed data. These two approaches are widely used using empirical relationships between LAI and individual band reflectance, a Vegetation Index (VI), and model inversion approach, which is based on the solution of the radiative transfer equations (Satapathy & Dadhwal 2005). An example of model inversion is the most widely used PROSAIL model, which includes both PROSPECT (Jacquemoud & F. Baret 1990) and SAIL models (Verhoef 1984).

The behavior of different VIs, such as NDVI, has been tested with the increase of the LAI during the growing seasons. At the beginning of the growing season, NDVI is sensitive to LAI. But when LAI exceeded 1.5 NDVI show low sensitivity. When tassels appeared, the reflectance of the canopy increased in red wavelengths, and NDVI remains virtually invariant (Gitelson et al. 2003).

The Visible Atmospherically Resistant Index (VARI) proposed by (Gitelson et al. 2003) has been tested in comparison with NDVI for estimating LAI of maize canopy through the different growing stages. Results showed a strong logarithmic relationship (R2 = 0.97) between VARI and LAI in the first stage when the LAI was from 0 to 6. Then, the relation became weaker when the tassels started to appear. According to Wulder (1998), LAI estimation of remote sensing vegetation indices is limited as the use of spectral values alone is not enough to estimate plant structural parameters. The accurate estimation needs bidirectional data, which remote sensing instruments cannot provide through one acquisition time (Jacquemoud et al. 1995). Furthermore, when LAI higher than 3, the relationship between most VIs, especially NDVI, became not a direct relationship. With the increase of LAI value, the vertical complexity of the stand also increases, and the measuring of LAI values from a nadir-viewing angle became more complex (Wulder 1998). In addition, the change in the leaf orientation from vertical to horizontal increases the ability of the plant to absorb light and decrease the reflectance, especially in the NIR region (Gitelson et al. 2003).

Another approach for retrieving LAI from remote sensing data is to invert the radiative transfer models, such as the PROSAIL model (Satapathy & Dadhwal 2005). In a study conducted by (Darvishzadeh et al. 2008), the potential of the PROSAIL model to predict LAI and leaf chlorophyll contents in heterogeneous Mediterranean grassland has been investigated. Results showed intermediate accuracy (R2=0.59, RMSE=0.18) for estimating LAI and limits the use of the PROSAIL radiative transfer model in heterogeneous conditions.

SPOT satellite spectral bands and six vegetation indices (GVI, DVI, IPVI, RVI, NDVI, SAVI, and LAI) were used as input parameters for yield prediction models. Among all the four bands and VIs, LAI was the most correlated to yield and gave the highest accuracy to predict yield (Noureldin et al., 2013; Aboelghar et al., 2014). Simulation models show a good correlation between first and second derivatives at 942.5 nm and leaf water content, while it has low sensitivity to leaf and canopy structure (Clevers et al., 2007). The first derivative of the slopes of the lines near bands 900nm and 970nm are well correlated with leaf water content (Danson et al., 1992). While water effect on nutrient stress can be investigated throughout the discrimination analysis of the visible and NIR reflectance of plant leaves (Christensen et al., 2005). In an experimental survey, corn leaves spectral reflectance were recorded in the red and near-infrared regions before and after irrigation applications. Results revealed a spectral response for corn leaves to irrigation applications. In addition, water-stressed plants absorbed less light in the visible and lighter in the NIR regions of the spectrum than unstressed plants (Genc et al., 2013).

MATERIALS AND METHODS

The study area named El-Salhiya project is located at Ismailia governorate and bounded by 31° 52' 36" & 32° 06' 26" longitudes and 30° 22' 02" & 30° 31' 16" latitudes (Fig.1). Two pivots selected at El-Salhiya project for this study No., 53 & 64. The climate is an arid Mediterranean type with an

average temperature of 21.4 Co. The original land of El-Salhiya area featured by dark yellowish-brown (moist) and light yellowish (dry), sandy, single grains, non-sticky, non-plastic and friable or lose characteristics had been changed to dark brown (moist) and dark yellowish-brown (dry), sandy loam, moderate medium sub-angular blocky structure, sticky, plastic and firm hard dry after 30 years of cultivation shown in figure (1).

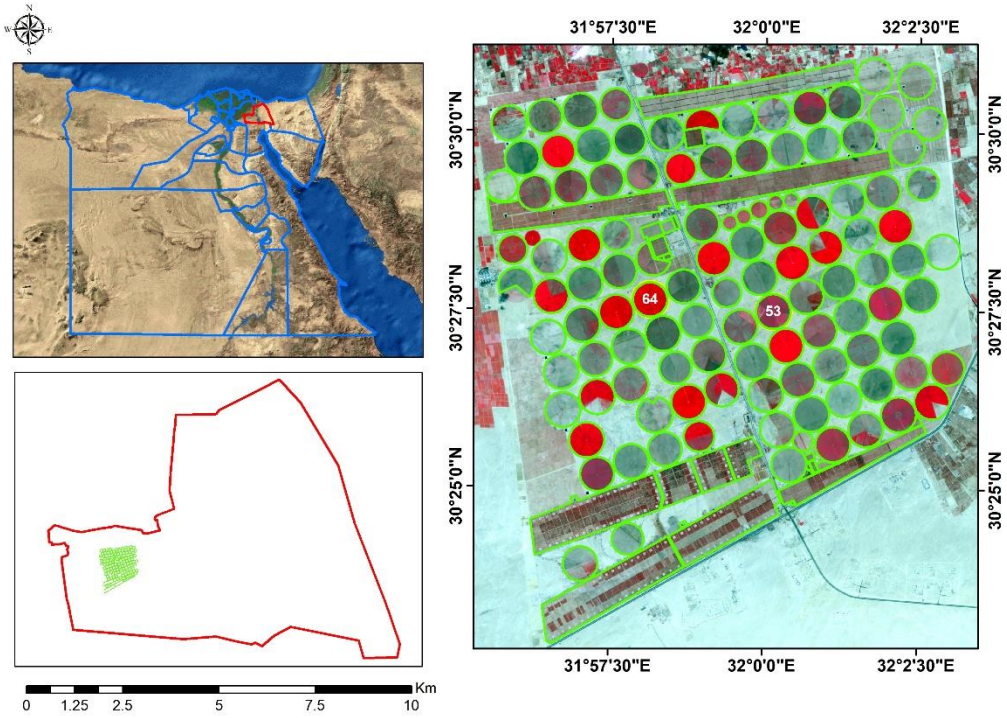

Figure 1: The study area illustrated on a Sentinel-2 image in a false-color composite

Field data collection:

Three *in-situ* measurements were conducted in the study area during the winter crop season of 2017. Moreover, it was scheduled to cover three different growth stages of the two crops (i.e., vegetative, flowering, and harvesting). The field visits were synchronized to the satellite passing days to capture the spectral signature of the two major crops existed in the study area (Table 1).

Table 1: Satellite passing days and *in-situ* measurements timetable

Growth Stage	Date
Vegetative stage	8 December 2016
Flowering stage	12 February 2017
Harvesting	22 March 2017

Two pivots were selected for the ground measurements cultivated by potato and wheat, where twenty-six points systematically selected for sampling LAI in at each pivot (Fig 2). The geographic coordinates at each sampling point recorded by a GPS receiver (Garmin e-Trex 20 receivers). Spectral measurements were taken by the ASD handheld spectroradiometer in the reflectance mode, i.e., the device records the reflected spectra from the target plant. In order to achieve that prior to each measurement, a white reference measurement was taken using the 20*20 cm standard spectralone. A number of five replicates spectra were recorded at each sampling point. These spectra were averaged to represent one sample in the statistical analysis and LAI estimation.

The number of leaves was counted at each sampling plant in addition to capturing a photo of this individual plant for LAI calculation using ENVI software (Fig. 3).

Maps of LAI were calculated for the three scenes of the Sentinel-2 images using the SNAP toolbox at the three growth stages, respectively, as illustrated in figures 4, 5, and 6.

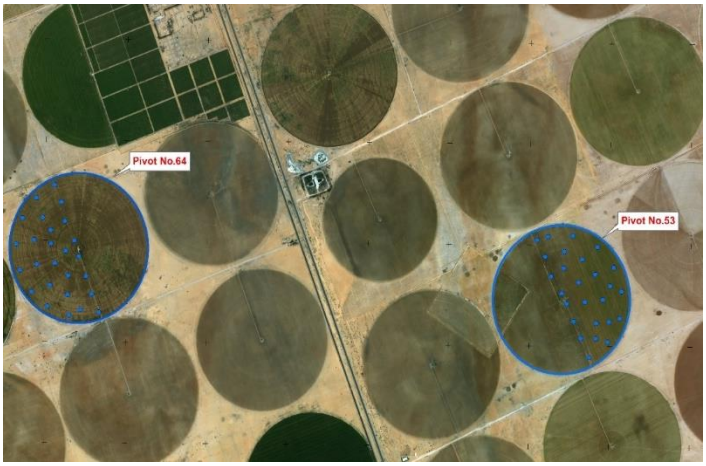

Figure 2: The studied pivots No., and samples points distribution in each pivote

Figure 3: LAI estimation for a plant leaves using ENVI software

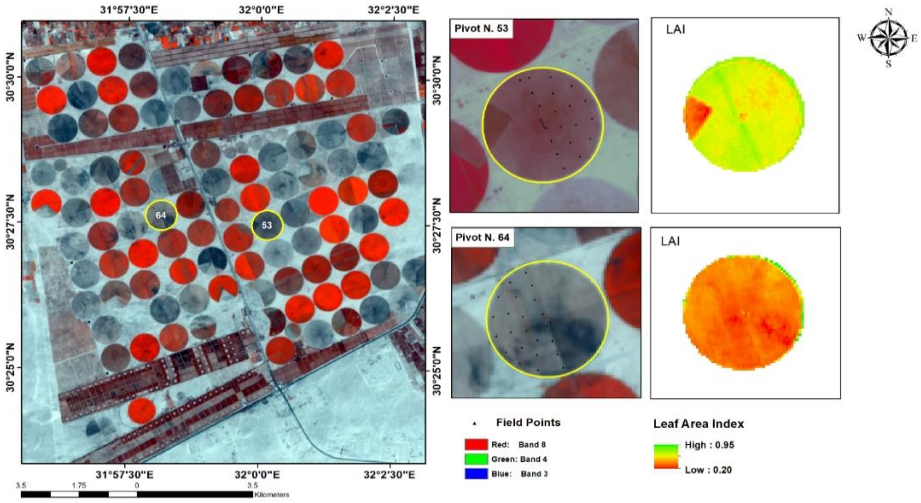

Figure 4: LAI at the vegetative growth stage.

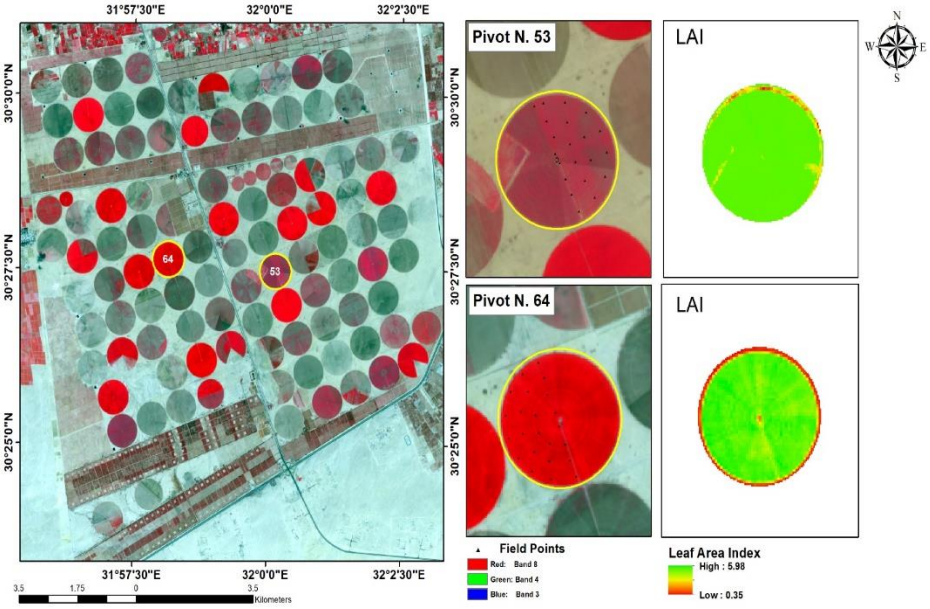

Figure 5: LAI at the flowering growth stage.

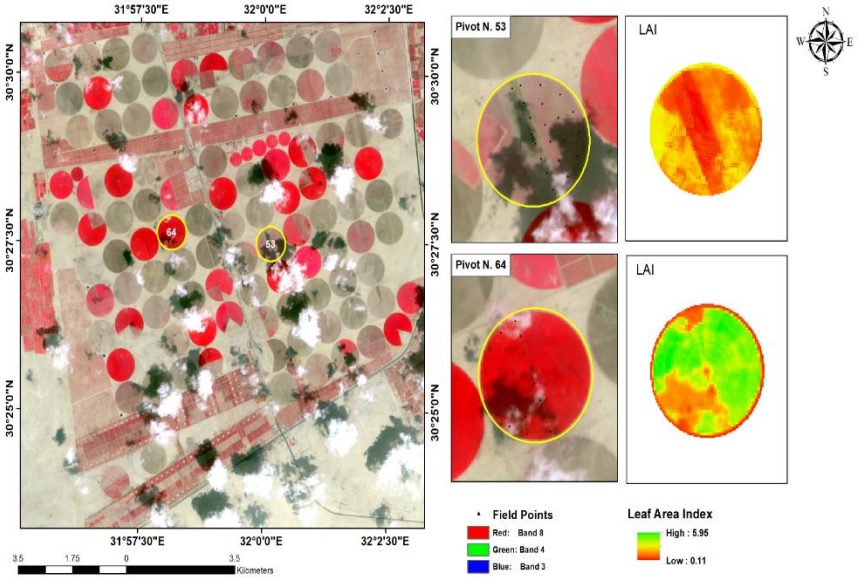

Figure 6: LAI at the harvest growth stage.

In addition to the Normalized Difference Vegetation Index (NDVI) using Equation 1 was calculated (Rouse et al., 1974)

$$NDVI = \frac{(\rho_{NIR} - \rho_{red})}{(\rho_{NIR} + \rho_{red})} \qquad \text{Equation.1}$$

Analysis of variance (ANOVA models) was applied to compare means from several populations, according to Mason et al. In addition to multiple comparisons of means frequently, involve preselected comparisons that address specific questions of interest to a researcher. Tukey's procedure was used for mean group comparison. Furthermore, the stepwise Multiple Linear Regression (MLR) analysis is used to predict the Coefficients to adapt the mapped values of LAI to measured LAI values, and Gauss-Newton neural nets were used for developing Neural Network NN. All materials and methods of this

study are summarized in the overall flowchart illustrated in fig (7)

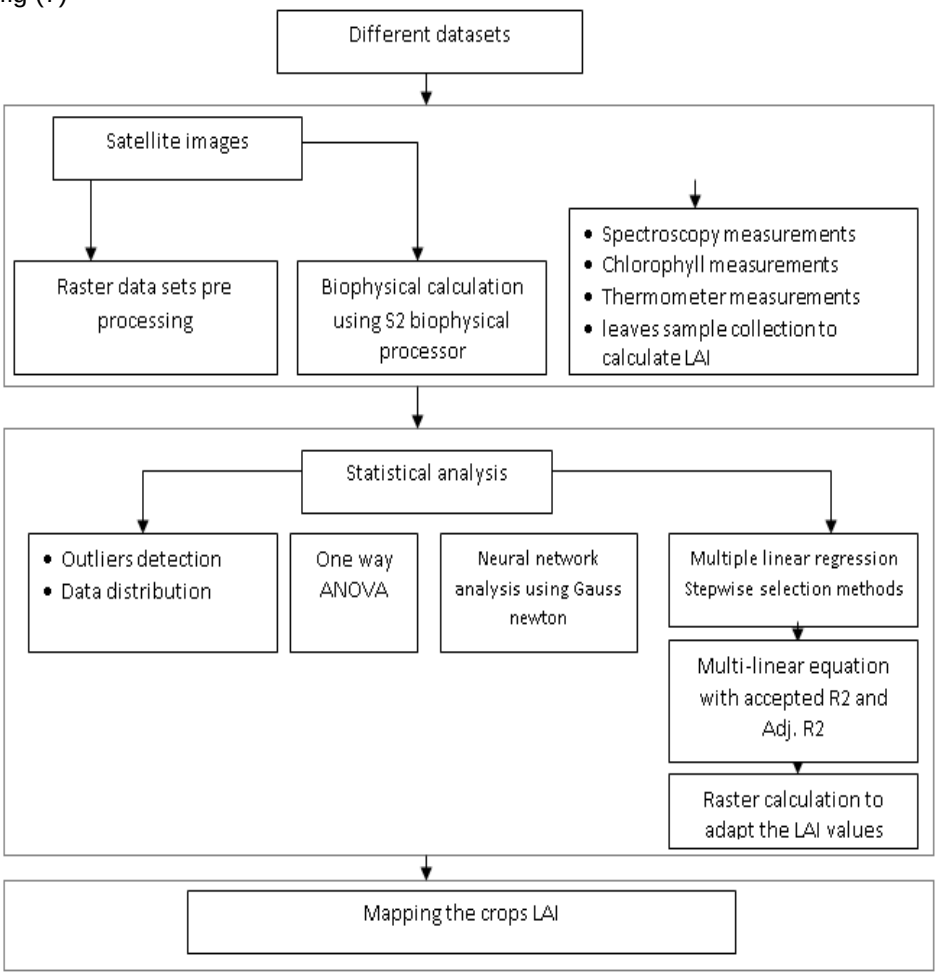

Figure 7: methodology flow diagram (after who ?)

RESULTS

3.1. In Situ measured LAI

The preliminary results of LAI measurements at flowering stage in both crops showed that the measured LAI values in potato pivot varied from 0.31 to 6.38 (m^2/m^2) with an average of 4.6 and standard deviation (SD) about 3.04 (m^2/m^2); this variation may be due to the great vegetative growth of potato crop at flowering stage. However, the variation decreased in the wheat pivot, where the measured LAI values varied from 2.35 to 5.81 (m^2/m^2) with an average of 4.2 and SD about 1.73 (m^2/m^2).

3.2. Estimated LAI from Sentinel-2

The results of estimated LAI at different growth stages in wheat and potato crops within the period (December and March) revealed that the average of LAI was generally higher at the initial stage in potato than wheat with an average 0.78 and 0.55 (m^2/m^2) respectively. During the flowering stage, the average LAI increased slightly from 2.6 to 3.5 (m^2/m^2) for both strategic crops. However, the variation slightly decreased approaching the harvest stage of potato at the end of March, while in the same period, it was slightly increased for wheat (Table 2).

A summary of the simple linear regression equations for Sentinel-2 reflectance bands and LAI at different growth stages is presented in figure 5. The correlation analyses between the leaf area of both crops and Sentinel-2 bands from the blue to the near-infrared revealed that NIR band had the highest correlation (r^2 = 0.83) followed closely by the red edge one and the red bands (r^2 = 0.72 and 0.66 respectively) then the green band (r^2 = 0.60).

The lowest correlation coefficient was reported for the third red edge, the first red edge and blue bands reaching 0.5, 0.28, and 0.05, respectively (Figure 8).

Table 2: Descriptive statistics of estimated LAI (m^2/m^2) from Sentinel-2 images

Descriptive Statistics	Vegetative stage		Flowering stage		3rd stage	
	Wheat	Potato	Wheat	Potato	Wheat	Potato
Count	26	26	26	26	26	26
Avg. (m^2/m^2)	0.55	0.78	4.2	4.6	4.5	3.1
Max (m^2/m^2)	0.95	0.91	5.81	6.38	5.95	5.95
Min (m^2/m^2)	0.2	0.2	2.35	0.31	2.1	0.11
SD	0.375	0.355	1.73	3.035	1.925	2.92

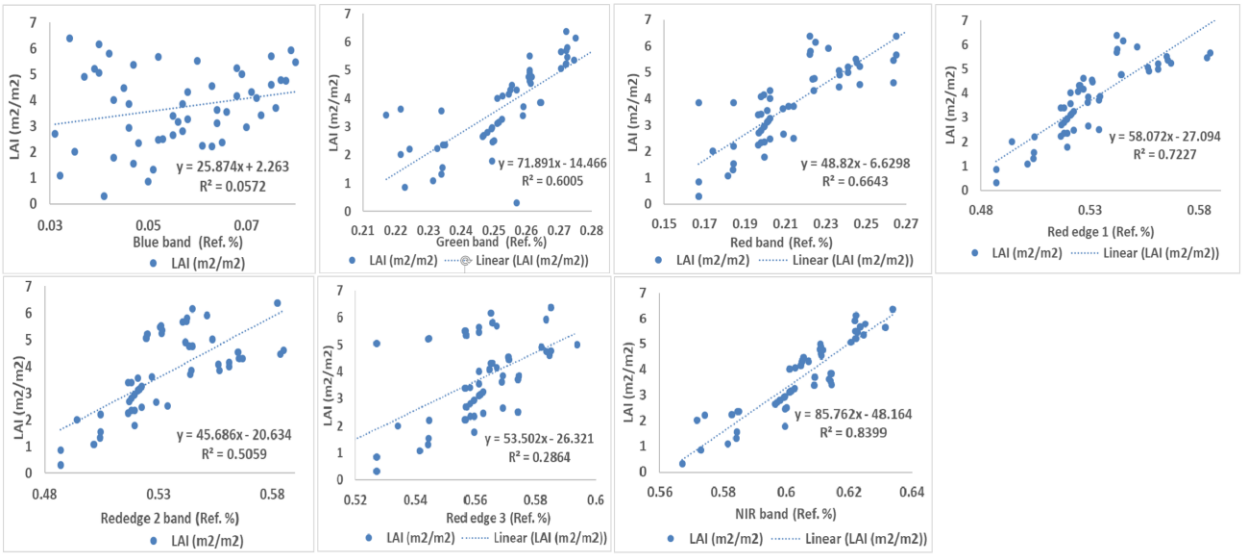

Figure 8: Correlation analyses between LAI and Sentinel-2 bands

The reflectance values of the red band varied from 0.17 to 0.26, while the reflectance values of the NIR band varied from 0.57 to 0.63. Also, the results revealed that NDVI values varied from 0.39 to 0.57 and 0.36 to 0.59 for wheat and potato, respectively. The selected datasets as an input of NNs included only red and near-infrared Sentinel-2 narrow bands, which are quite similar to the Landsat and Rapideye bands and NDVI.

The efficacy of the chosen minimum datasets was evaluated for their capacity to estimate potato and wheat LAI by performing MLR analyses of each minimum data set against the measured LAI. Also, the MLR analysis was used to improve the selection of the different datasets of Sentinel-2 narrow bands used as input layers of the neural network to predict the leaf area index.

The results from the estimated equations were used to map the wheat and potato LAI from Sentinel-2 for each growth stage, as illustrated in figure 9. Maps of calculated LAI for the three scenes of the Sentinel-2 images using the SNAP toolbox at the three growth stages showed in Figure 9.

3.3. Predicted LAI from using MLR and ANNs algorithms

Results of the calculations and the toolbox compared statistically with different statistical tests since the correlation between the calculated from field samples and estimated from satellite data was tested and showed a high positive correlation with value 0.83 results of correlation analysis illustrated in figure (10) and table (3). Validation was applied using in situ measured LAI, and the result shows that correlation between the measured LAI and calculated LAI for the three different growth stages was significantly presented in table 3.

Moreover, both data sets have been tested for the differences between the two crops potato and wheat that assigned to dates December 2016 and March 2017 represents middle and late growth stage, respectively. Results of either mapped or

calculated leaf area index were significantly different from the middle growth stage to late stages with higher values correspond to the middle growth stage due to high vegetative growth.

Finally, statistics MLR using the stepwise method was applied on the datasets to estimate the LAI from satellite image red, NIR spectral response, and NDVI. The results showed that a combination of full factorial to estimate the LAI was significant with R2 and Adj. R2 0.89 and 0.87, respectively, see figure (11) and table (4).

The artificial structure of NNs for LAI estimation showed varied numbers of the neuron input layers, and neuron-hidden layers with one output layer represent predicted LAI, as shown in (Figure 8). The network included three layers, namely, a single input layer with seven input nodes, which represent the Red reflectance, NIR reflectance and NDVI measured at 26 different spots from each Pivot. Moreover, the Gauss-Newton algorithm used for developing Neural Network NN to estimate LAI values using the satellite Red, NIR spectral response, and NDVI with seven nodes with maximum iteration 75 (Fig. 12).

The results indicated that using NNs is better for LAI satellite values adaption to real values and showed high R2 0.93 between estimated and measured LAI, which is higher than the MLR shown in figures (13 and 14) and table (5).

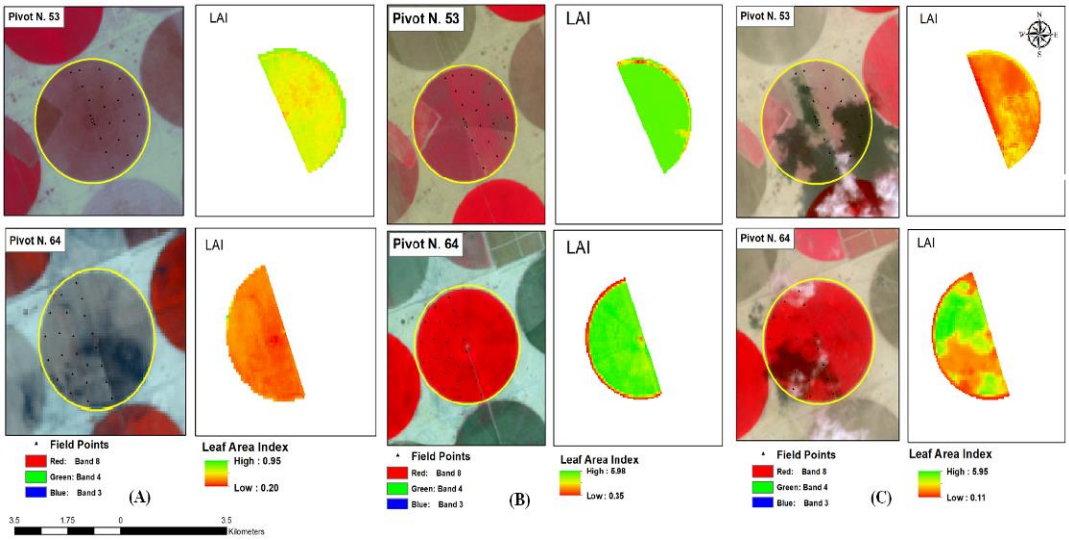

Figure 9: Maps of calculated LAI from Sentinel-2 at three growth stages of the crop, (A) Vegetative; (B) Flowering, and (C) Harvesting stages

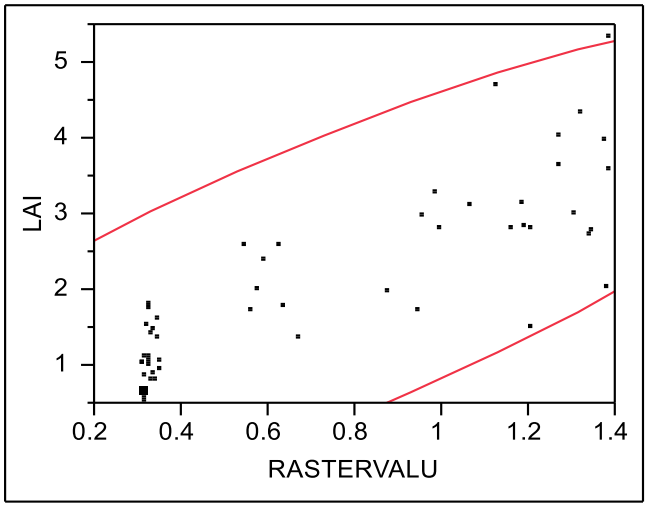

Figure 10: Correlation analysis of calculated LAI from field data and mapped from Sentinel-2 image using MLR

Table 3: Correlation analysis of calculated LAI from Field and SNAP LAI

Variable	Mean	Standard deviation	Correlation	Significant Probability
SNAP LAI	1.926197	0.420712	0.83	<.0001*
LAI	2.048103	1.195406		

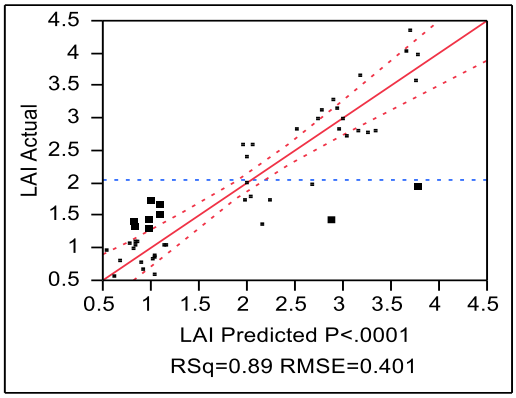

Figure 11: MLR predicted LAI vs. field-measured LAI

Table 4: Parameter Estimates of the MLR model

Term	Est.	Std Err	t Ratio	Prob>|t|
Intercept	-0.21	0.73	-0.29	0.7747
Red	2.47	2.66	0.93	0.3611
NIR	2.57	6.61	0.39	0.7000
(NDVI -0.74472)*(fcover-0.28152)	31.99	15.33	2.09	0.0447*
NDVI	0.081	5.46	0.01	0.9881
(Red-0.74472) *(NDVI -0.32228)	9.52	21.68	0.44	0.6633
(NIR-0.28152) *(NDVI -0.32228)	-95.92	39.67	-2.42	0.0213*
(Red-0.74472) *(NIR-0.28152) * (NDVI - 0.32228)	-38.43	27.02	-1.42	0.1643

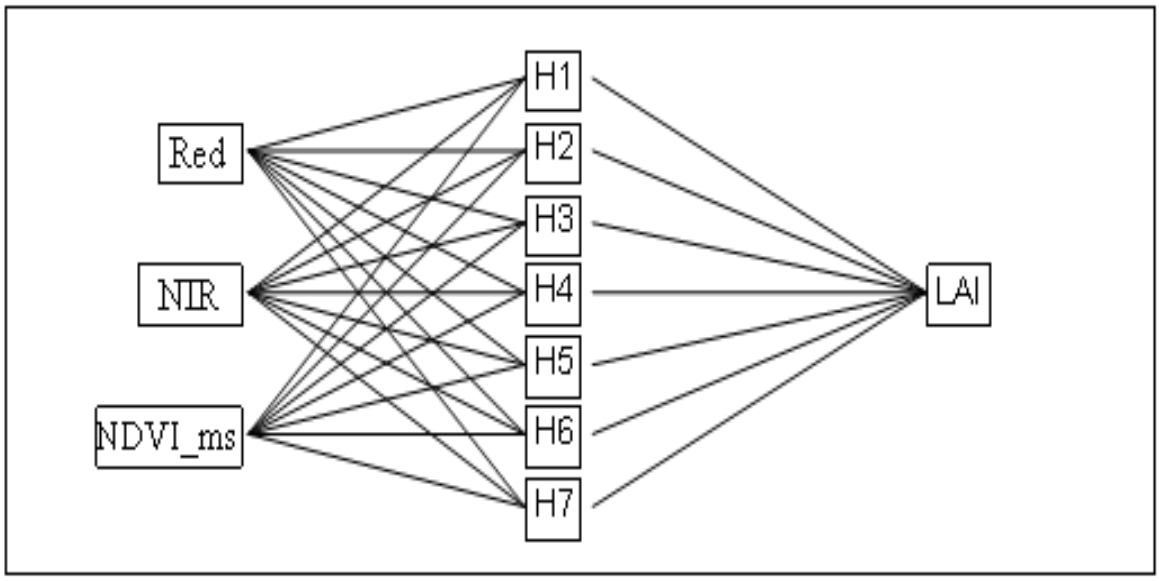

Figure 12: Neural Network systematic graph.

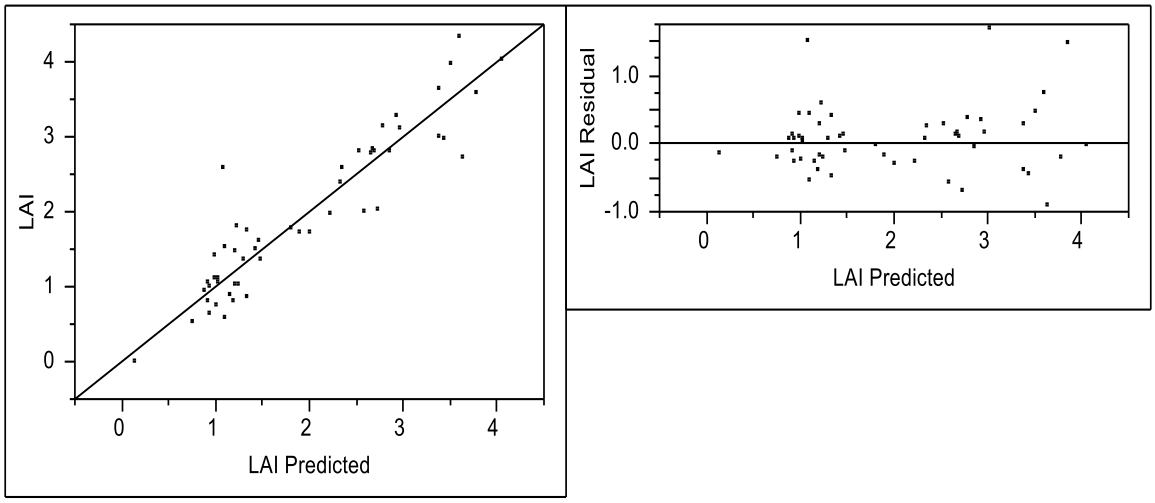

Figure 13: Correlation analysis of calculated LAI from Field data and mapped from satellite image

Table 5: Correlation analysis of calculated LAI from Field and mapped LAI using NN

Variable	Mean	Standard deviation	Correlation	Significant Probability
Mapped LAI	1.926197	0.420712	0.92	<.0001*
LAI	2.25	1.218352		

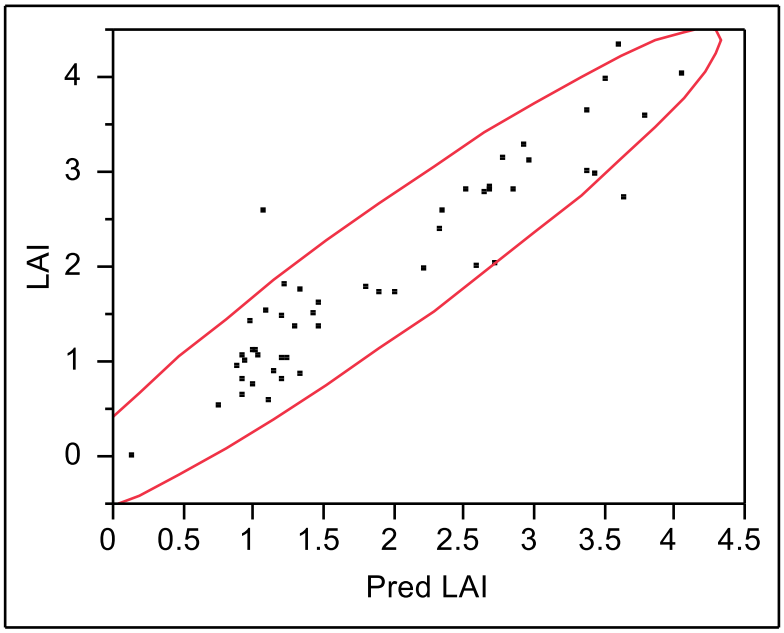

Figure 14: Correlation analysis of the calculated LAI from field data and mapped from satellite image using Gauss-Newton NN

CONCLUSION

According to the results of our investigation, using Sentinel-2 satellite imagery is essentially significant for mapping and estimation leaf area index LAI for field crops. Moreover, ANN is a promising approach for estimation of leaf area index LAI from Sentinel-2 data since NN shows higher R2 than MLR. However, MLR is most suitable for research purposes because it has advantages to show relationships between predictors and predicted outcomes and influence of each predictor factor in the developed model.

CONFLICT OF INTEREST

The authors declared that the present study was performed in the absence of any conflict of interest.

ACKNOWLEDGMENT

The authors would like to thank National Authority for Remote Sensing and Space Sciences, Egypt for funding and offering its resources to perform this study, within the framework of the project entitled "Retrieval of vegetation physiological parameters using remote sensing data".

AUTHOR CONTRIBUTIONS

Eslam Farg; Khaled A. Abutaleb; S. M. Arafat Mohamed M. El Sharkawy; and Mohsen Nabil designed and performed the experiments and also wrote the manuscript. All authors read and approved the final version.

REFERENCES

Aboelghar, M., Ali, A. R., & Arafat, S. (2014). Spectral wheat yield prediction modeling using SPOT satellite imagery and leaf area index. Arabian Journal of Geosciences, 7(2), 465-474.

Blanco, F. F., & Folegatti, M. V. (2003). A new method for estimating the leaf area index of cucumber and tomato plants. Horticultura Brasileira, 21(4), 666-669.

Christensen, L. K., Upadhyaya, S. K., Jahn, B., Slaughter, D. C., Tan, E., & Hills, D. (2005). Determining the influence of water deficiency on NPK stress discrimination in maize using spectral and spatial information. Precision Agriculture, 6(6), 539-550.

Danson, F. M., Steven, M. D., Malthus, T. J., & Clark, J. A. (1992). High-spectral resolution data for determining leaf water content. International Journal of Remote Sensing, 13(3), 461-470.

Darvishzadeh, R., Skidmore, A., Schlerf, M., Atzberger, C., Corsi, F., & Cho, M. (2008). Estimation of leaf area index and chlorophyll for a Mediterranean grassland using hyperspectral data. The International Archives of the Photogrammetry, Remote Sensing and Spatial Information Sciences, XXXVII, Part B, 7, 471-478.

Deering, D. W. (1978). Rangeland reflectance characteristics measured by aircraft and spacecraft sensors. Deering.

Genc, L., Inalpulat, M., Kizil, U., Mirik, M., Smith, S. E., & Mendes, M. (2013). Determination of water stress with spectral reflectance on sweet corn (Zea mays L.) using classification tree (CT) analysis. Zemdirbyste-Agriculture, 100(1), 81-90.

Gitelson, A. A., Gritz, Y., & Merzlyak, M. N. (2003). Relationships between leaf chlorophyll content and spectral reflectance and algorithms for non-destructive chlorophyll assessment in higher plant leaves. Journal of plant physiology, 160(3), 271-282.

Gong, P., Pu, R., Biging, G. S., & Larrieu, M. R. (2003). Estimation of forest leaf area index using vegetation indices derived from Hyperion hyperspectral data. IEEE transactions on geoscience and remote sensing, 41(6), 1355-1362.

Jacquemoud, S., & Baret, F. (1990). PROSPECT: A model of leaf optical properties spectra. Remote sensing of environment, 34(2), 75-91.

Jacquemoud, S., Baret, F., Andrieu, B., Danson, F. M., & Jaggard, K. (1995). Extraction of vegetation biophysical parameters by inversion of the PROSPECT+ SAIL models on sugar beet canopy reflectance data. Application to TM and AVIRIS sensors. Remote sensing of environment, 52(3), 163-172.

Jonckheere, I., Fleck, S., Nackaerts, K., Muys, B., Coppin, P., Weiss, M., & Baret, F. (2004). Review of methods for in situ leaf area index

determination: Part I. Theories, sensors, and hemispherical photography. Agricultural and forest meteorology, 121(1), 19-35.

Mason R. L., Gunst R. F., and Hess J. L. (2003). Statistical design and analysis of experiments with applications of engineering and science, 2nd edition, John Willey and Sons Hoboken, New Jersey, USA.

Noureldin, N. A., Aboelghar, M. A., Saudy, H. S., & Ali, A. M. (2013). Rice yield forecasting models using satellite imagery in Egypt. The Egyptian Journal of Remote Sensing and Space Science, 16(1), 125-131.

Pu, R., Gong, P., Biging, G. S., & Larrieu, M. R. (2003). Extraction of red edge optical parameters from Hyperion data for estimation of forest leaf area index. IEEE Transactions on Geoscience and Remote Sensing, 41(4), 916-921.

Rouse Jr, J. W. (1974). Monitoring the vernal advancement and retrogradation (green wave effect) of natural vegetation.

Satapathy, S., & Dadhwal, V. K. (2005). Principal component inversion technique for the retrieval of leaf area index. Journal of the Indian Society of Remote Sensing, 33(2), 323-330.

Verhoef, W. (1984). Light scattering by leaf layers with application to canopy reflectance modeling: the SAIL model. Remote sensing of environment, 16(2), 125-141.

Wulder, M. (1998). Optical remote-sensing techniques for the assessment of forest inventory and biophysical parameters. Progress in Physical Geography, 22(4), 449-476.

Wulder, M. A., LeDrew, E. F., Franklin, S. E., & Lavigne, M. B. (1998). Aerial image texture information in the estimation of northern deciduous and mixed wood forest leaf area index (LAI). Remote Sensing of Environment, 64(1), 64-76.